Video Article

# *In Vivo* Multimodal Imaging and Analysis of Mouse Laser-Induced Choroidal Neovascularization Model

Symantas Ragauskas[1], Eva Kielczewski[2], Joseph Vance[2,3], Simon Kaja[1,4], Giedrius Kalesnykas[1]

[1]Experimentica Ltd.

[2]Leica Microsystems

[3]Spective LLC

[4]Department of Ophthalmology, Stritch School of Medicine, Loyola University Chicago

Correspondence to: Giedrius Kalesnykas at giedrius.kalesnykas@experimentica.com

URL: https://www.jove.com/video/56173
DOI: doi:10.3791/56173

Keywords: Neurobiology, Issue 131, Laser-induced choroidal neovascularization, mouse CNV, age-related macular degeneration, angiogenesis, *in vivo* imaging, optical coherence tomography, SD-OCT

Date Published: 1/21/2018

Citation: Ragauskas, S., Kielczewski, E., Vance, J., Kaja, S., Kalesnykas, G. *In Vivo* Multimodal Imaging and Analysis of Mouse Laser-Induced Choroidal Neovascularization Model. *J. Vis. Exp.* (131), e56173, doi:10.3791/56173 (2018).

## Abstract

Laser-induced choroidal neovascularization (CNV) is a well-established model to mimic the wet form of age-related macular degeneration (AMD). In this protocol, we aim to guide the reader not simply through the technical considerations of generating laser-induced lesions to trigger neovascular processes, but rather focus on the powerful information that can be obtained from multimodal longitudinal *in vivo* imaging throughout the follow-up period.

The laser-induced mouse CNV model was generated by a diode laser administration. Multimodal *in vivo* imaging techniques were used to monitor CNV induction, progression and regression. First, spectral domain optical coherence tomography (SD-OCT) was performed immediately after the lasering to verify a break of Bruch's membrane. Subsequent *in vivo* imaging using fluorescein angiography (FA) confirmed successful damage of Bruch's membrane from serial images acquired at the choroidal level. Longitudinal follow-up of CNV proliferation and regression on days 5, 10, and 14 after the lasering was performed using both SD-OCT and FA. Simple and reliable grading of leaky CNV leasions from FA images is presented. Automated segmentation for measurement of total retinal thickness, combined with manual caliber application for measurement of retinal thickness at CNV sites, allow unbiased evaluation of the presence of edema. Finally, histological verification of CNV is performed using isolectin GS-IB4 staining on choroidal flatmounts. The staining is thresholded, and the isolectin-positive area is calculated with ImageJ.

This protocol is especially useful in therapeutics studies requiring high-throughput-like screening of CNV pathology as it allows fast, multimodal, and reliable classification of CNV pathology and retinal edema. In addition, high resolution SD-OCT enables the recording of other pathological hallmarks, such as the accumulation of subretinal or intraretinal fluid. However, this method does not provide a possibility to automate CNV volume analysis from SD-OCT images, which has to be performed manually.

## Video Link

The video component of this article can be found at https://www.jove.com/video/56173/

## Introduction

The first successful attempt to mimic the pathology of human CNV in rodents was demonstrated almost three decades ago with a krypton laser in Long-Evans rats[1]. Thereafter, a krypton laser was used to break Bruch's membrane in the most popular mouse strain, C57BL/6J[2,3,4]. The success rate of CNV induction was verified with FA and histological stains. A rapid development of noninvasive imaging modalities, such as OCT, fostered the growth of the field of rodent preclinical models. The ability to monitor morphological changes in the retina at multiple time points in the same eye significantly contributes to the reduction of animal use, and increases efficiency in experimental studies. Histological evaluation of CNV lesions is rather straightforward, and requires labeling of abnormal vascular growth around the site of laser administration, image acquisition, and area/volume estimation using an image analysis software. In contrast, *in vivo* imaging modalities introduce more complex analyses of CNV pathology and its interpretation.

Here we present a simple and relatively fast method to grade induction, progression, and regression of CNV using FA, SD-OCT, and the automated segmentation method in the mouse laser-induced CNV model.

Copyright © 2018 Journal of Visualized Experiments

## Protocol

All animals were treated in accordance with the ARVO Statement for the Use of Animals in Ophthalmic and Vision Research and the EC Directive 86/609/EEC for animal experiments, using protocols approved and monitored by the Animal Experiment Board of Finland.

## 1. Laser-induced mouse CNV model [5]

1. Inspect the eyes of the animal macroscopically for any abnormalities.
2. Weigh the mouse.
3. Calculate and prepare an appropriate amount of anesthetics to use, based on the weight of the animal, *e.g.* a mixture of medetomidine (1 mg/kg), ketamine (75 mg/kg), and distilled water (0.9% NaCl solution) at a ratio of 1:1.5:2.5, or ketamine (40-75 mg/kg), xylazine (5 mg/kg), and distilled water (0.9% NaCl solution) at a ratio of 1:2.5:1; for a 20 g mouse, inject 0.1 mL of mixture.
4. Inject anesthetic intraperitoneally.
5. Place mouse back into the cage and wait until animal is anesthetized. Confirm the mouse is properly anesthetized by lack of a pedal reflex.
6. Ensure the use of laser safety personal protective equipment.
7. Turn on a slit lamp and a 532 nm diode laser.
8. Remove the mouse from the cage and place on the heating pad.
9. Apply one drop of Tropicamide for pupillary dilation. Wait for 3-5 min for full (3 mm) pupillary dilation.
10. Place the mouse on the stage of the slit lamp.
11. Place one drop of opthalmic liquid gel on a coverslip to applanate the cornea.
12. Orient the mouse eye with the optic nerve head in the center.
13. Set the laser power to 100 mW, the duration to 100 ms, and the spot size to 50 µm.
14. Focus the laser beam on the retinal pigment epithelium (RPE).
15. Make three laser shots into one eye by avoiding retinal blood vessels ideally at the 4, 8, and 12 o'clock positions around the optic nerve, respectively. Inspect the fundus of the eye after all laser shots for absence of retinal bleeding. The contralateral eye serves as a non-lasered control.
16. Discard the coverslip and place mouse back on the heating pad.
17. Apply one drop of PEG gel drops on both eyes.

## 2. SD-OCT [6,7]

1. Place the mouse into the rodent alignment stage, and immobilize the head.
2. Align the lens of the SD-OCT system (*e.g.*, Bioptigen/Leica Envisu R2200) to face the eye for *in vivo* imaging using X- and Y-stage controllers.
3. Perform SD-OCT scans to verify breaks of Bruch's membrane: once the SD-OCT scans the whole eye, manually move the reference line on the lasered sites. Breaks of Bruch's membrane should be clearly visible in lasered areas (see **Figure 1**).

## 3. Fluorescein angiography [7,8,9]

1. Remove mouse with the holder, and place it on the FA system (*e.g.*, Heidelberg Spectralis HRA2).
2. Focus at laser burn areas of the fundus of the eye using infrared reflectance mode with the head of the optic nerve in the middle of the viewing window.
3. Inject 0.1 mL of 5% fluorescein sodium salt for a 20 g mouse subcutaneously or intraperitoneally.
4. Focus on the choroidal level.
5. Take an image from the choroidal focus level.
6. Re-focus at the retinal level and take an image.
7. Wait for 30 s and repeat steps 3.4-3.6.
8. Remove the mouse from the holder and place it on the heating pad.
9. Reverse anesthesia by α2-antagonist for medetomidine, atipamezole (0.5 mg/kg, i.p.), or wait for animal recovery from anesthesia.
10. Repeat *in* vivo SD-OCT and FA imaging in anesthetized animals on the follow-up days 5, 10, and 14.

## 4. CNV Grading

1. Grade the damage of Bruch's membrane from OCT images and choroidal FA images taken immediately after the lasering on day 0 as following:
   0 - Bruch's membrane was not damaged
   1 - successful damage of Bruch's membrane
2. Grade the presence of CNV from lasered spots that had leakage as observed by comparing dynamics of fluorescein signal in a series of retinal FA images as following:
   0 - normal appearance of retina
   0.5 - faint staining of leakage
   1.0 - leaky CNV areas
   Note: Use the OCT imaging for additional confirmation of CNV or in questionable FA where the presence of intraretinal fluid in OCT images would suggest CNV grading.

## 5. Retinal Thickness Measurements

1. Use an automated segmentation software for retinal thickness measurements. Ensure that the total retinal thickness is considered, as the thickness of all layers from nerve fiber layer to RPE (healthy measurement sites), or to an imaginary line connecting RPE around the site of damage (lasered sites) (see also **Figure 7**).

## Representative Results

A bubble or subretinal bleeding immediately after lasering is not always visible. Therefore, SD-OCT is particularly important to verify damage of Bruch's membrane. **Figure 1** shows an example of OCT imaging at different time points after laser administration.

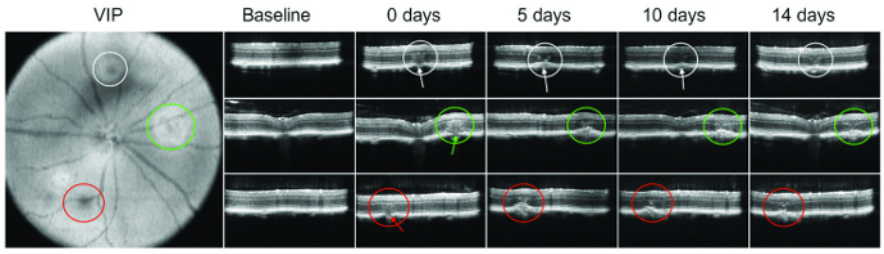


**Figure 1: OCT en face view of eye fundus (VIP image) shows three lasered areas outlined in white, green and red circles.** OCT B-scan images were taken prior the lasering (baseline), immediately after the lasering to verify a break of Bruch's membrane (0 days, arrows point to the site of damage), and 5, 10 and 14 days after laser administration. As can be seen from the area outlined in white (first row of images), CNV did not develop at later timepoints. The area outlined in green and red developed CNV, which was detected on follow-up day 5. However, at the 10 and 14 day timepoints, these CNV lesions regressed. Please click here to view a larger version of this figure.

**Figures 2 and 3** show serial imaging using FA, which confirmed successful damage of Bruch's membrane in all three spots on day 0 in a male 10-week-old C57BL/6jRj mouse.

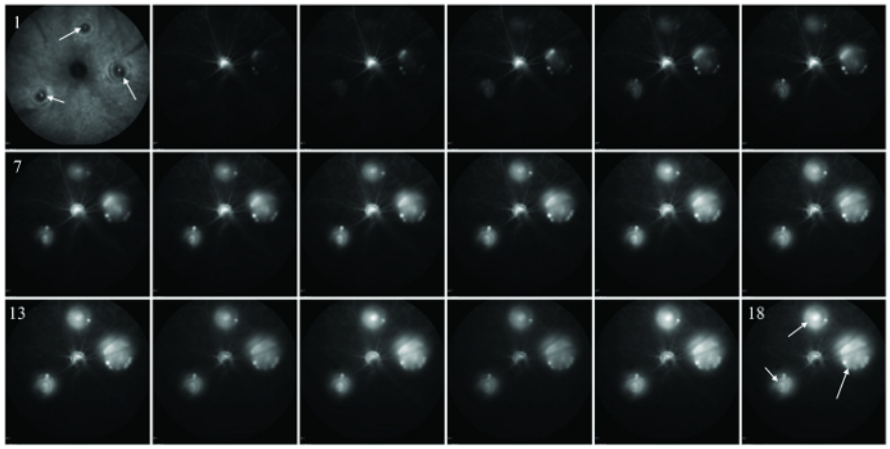


**Figure 2: Serial FA imaging taken every 20 s (images 1 through 18) at the choroidal level immediately after laser administration.** White arrows in image 1 point to lasered sites, which show fluorescein leakage at later timepoints (white arrows in image 18). Please click here to view a larger version of this figure.

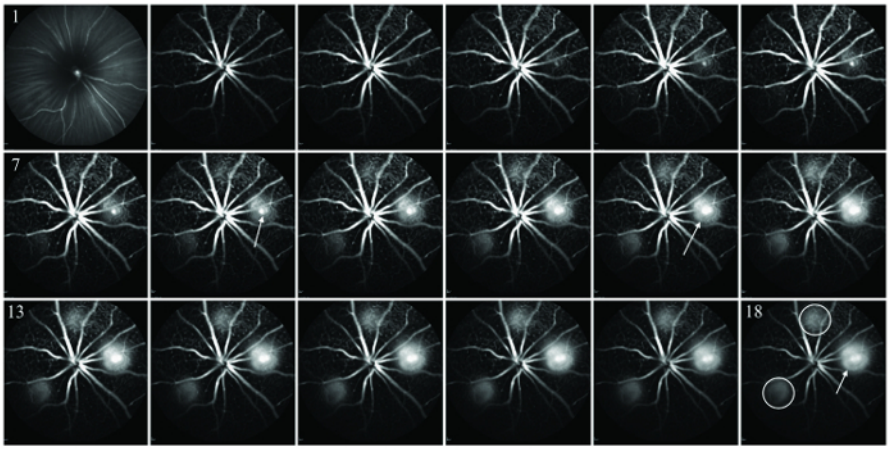


**Figure 3: Serial FA imaging taken every 20 s (images 1 through 18) at the retinal level immediately after laser administration.** CNV area that has fluorescein leakage and a grading of 1 (leaky CNV) is pointed out by the white arrow in image 18. Note an increasing intensity, as well as fluorescein positive area, during the timecourse of FA imaging (white arrow in images 8 and 11). Two areas outlined in white in the image 18 were graded as having a faint FA signal (grading 0.5). Please click here to view a larger version of this figure.

In addition to the grading of CNV pathology, SD-OCT is also useful to reveal additional information in the lesion site, *e.g.*, presence of subretinal fluid, edema, and CNV regression. **Figure 4** shows the main pathological hallmarks of laser-induced CNV in mice.

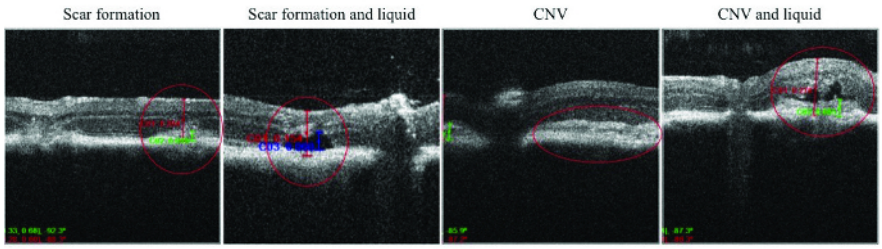


**Figure 4: Spectral Domain Optical Coherence Tomography Imaging of CNV pathology.** SD-OCT provides a detailed CNV pathology within retinal tissue, as can be seen from these representative images on scarring tissue, CNV formation, and liquid accumulation. Please click here to view a larger version of this figure.

Macular edema is one of the main pathological hallmarks of wet form AMD in humans. In the laser-induced CNV model, retinal thickness can be evaluated using automated segmentation. Manual measurement of selected lasered sites is required to measure retinal thickness at the site of CNV. **Figure 5** shows an example of a report generated after automated segmentation.

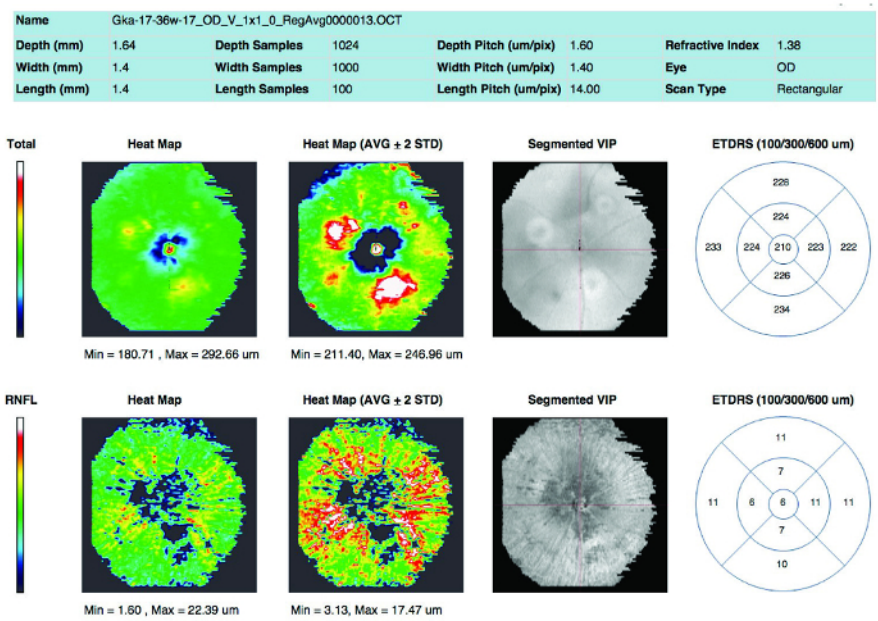


**Figure 5: Quantification of retinal thickness.** Retinal thickness as measured by automated segmentation Please click here to view a larger version of this figure.

The use of automated segmentation is a fast way to provide an overview of retinal thickness (**Table 1**). **Figures 6A** and **6B** show representative examples of automated segmentation from a healthy retinal area and from the retinal area with CNV pathology, respectively. Despite minor inaccuracies found in distinguishing individual retinal layers, overall, the software reliably recognizes the total retinal thickness in pigmented mice.

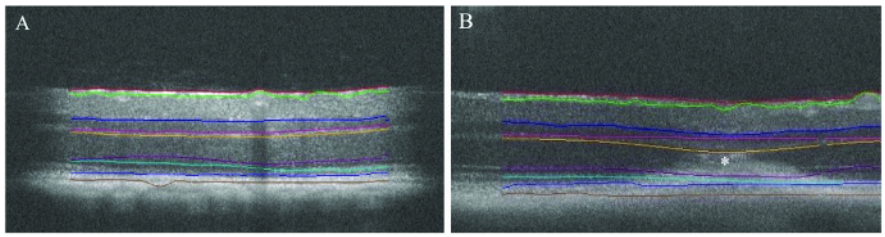


**Figure 6: Automated segmentation of retinal layers.** Automated segmentation of healthy retinal area (**A**) and retinal area containing CNV (asterisk in image **B**). Please click here to view a larger version of this figure.

In order to evaluate the retinal thickness at lasered areas, each lasered area was measured manually as following: the total retinal thickness was considered as the thickness of all layers from nerve fiber layer to the imaginary line connecting RPE around the site of damage (**Figure 7** and **Table 1**).

| Area | Day 5 | Day 10 | Day 14 |
|---|---|---|---|
| Total retinal thickness, µm | 218±7.8 | 220±7.2 | 221±9.8 |
| Lasered area 1 | 200 | 204 | 214 |
| Lasered area 2 | 226 | 217 | 220 |
| Lasered area 3 | 222 | 223 | 227 |
| Data are presented as mean±SD | | | |

**Table 1. Total retinal thickness and retinal thickness at CNV sites during a 14-day follow-up as determined by automated segmentation using inVivoDiver software (v. 3.0.8).**

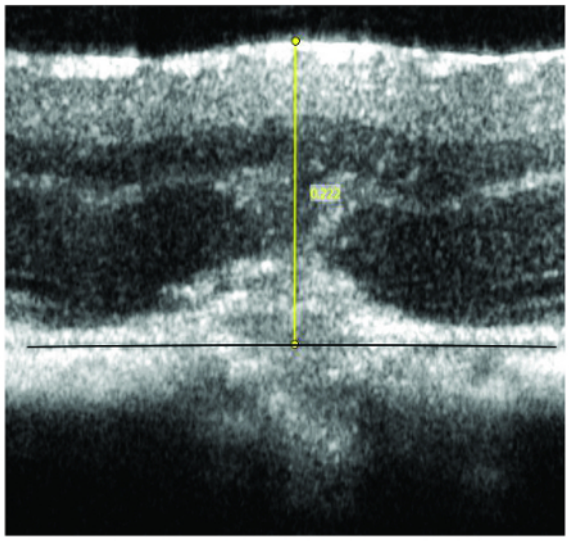

**Figure 7: Manual measurement of retinal thickness at lasered area with CNV pathology.** Yellow line indicates the total retinal thickness from nerve fiber layer to an imaginary RPE layer (black line) at the site of laser administration. Please click here to view a larger version of this figure.

Histologically, the CNV lesions were confirmed using isolectin GS-IB4 labeling (**Figure 8A**). Image analysis software Image J was used to calculate the area of CNV lesion (**Figure 8B**).

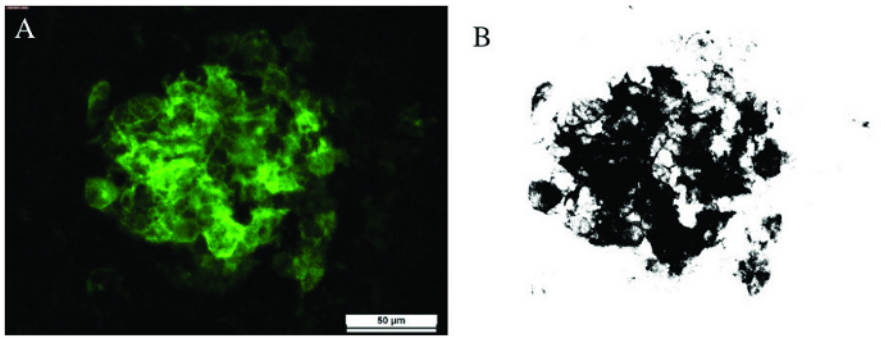


**Figure 8: Histological analysis.** Histological stain of CNV lesion from choroidal flatmount (in green, **A**) can be quantified using thresholding in Image J (**B**). The scale bar for **A** is 50 µm. Please click here to view a larger version of this figure.

## Discussion

Multimodal imaging offers valuable tools for CNV pathology evaluation. Here we presented an imaging protocol consisting of FA, SD-OCT, and automatic segmentation for the quick, reproducible, and reliable evaluation of CNV pathology. A break of Bruch's membrane after laser administration was confirmed. In addition, the use of SD-OCT at this stage also allowed immediate visualization of possible intraretinal and subretinal hemorrhages, which may confound the interpretation of results. Retinal leaks were graded based on the fluorescein signal from FA images. The use of SD-OCT provided a more detailed description of CNV pathology. Moreover, longitudinal SD-OCT analysis at various time points throughout the follow-up period highlighted temporal differences in the pathology that would remain elusive if relying on FA alone.

Total retinal thickness was measured using automated segmentation. Retinal thickness at sites CNV was induced was manually measured. The histological evaluation of choroidal flatmount is verified, and the area of neovascularization is measured using image analysis software Image J.

The proper transparency of the visual axis is critical for successful performance of the presented protocol. Dryness of the cornea and formation of cataracts are the main factors involved in troubleshooting. Therefore, once the mouse gets anesthetized, the eyes should be constantly hydrated with artificial tears or gel to maintain proper hydration of the cornea. The proposed protocol should be performed preferentially within 10 min from the induction of anesthesia. Extended anesthesia time may cause the formation of cataracts and prevent *in vivo* imaging.

The described protocol is limited to observational grading of CNV progression based on vascular leaks at the level of the retina. Quantitative assessment of retinal leak can be added using Heidelberg Spectralis software, which allows the delineation of the area of the leak, and provides quantitative data on the region of interest. In addition, Sulaiman and colleagues (2015) recently proposed a calculation of CNV volume from *in vivo* acquired OCT images using the ellipsoid method[10]. The ellipsoid model most likely introduces bias toward overestimation of volume of lesions as CNV in most cases has an irregular shape. However, high correlation between volume measurements from confocal analysis

of histological samples and proposed ellipsoid quantification from OCT images provides evidence that the method is a valuable tool for the quantitative evaluation of CNV volume[10].

To conclude, we believe the presented combination of different *in vivo* imaging modalities, together with automated segmentation and histological analysis, provides reproducible and reliable evaluation of CNV pathology in preclinical studies. The method could be particularly useful for proof of concept therapeutic intervention studies.

## Disclosures

The author Symantas Ragauskas, Ph.D. is an employee (research scientist) and shareholder of Experimentica Ltd. that offers contract research services employing the preclinical CNV model used in this Article.

The author Eva Kielczewski is an employee (research applications engineer, OCT) of Leica Microsystems that produces SD-OCT systems used in this Article.

The author Joseph Vance is an employee (NA OCT Sales Director) of Leica Microsystems that produces SD-OCT systems used in this Article. Joseph Vance is also president and managing director of Spective, LLC.

The author Simon Kaja, Ph.D. is consultant Chief Scientific Officer and shareholder of Experimentica Ltd., a preclinical contract research organization that offers contract research services, incl. the preclinical CNV model used in this article. Simon Kaja, Ph.D. is also CEO of K&P Scientific, LLC, a life sciences consulting firm, and serves as the Dr. John P. and Therese E. Mulcahy Endowed Professor in Ophthalmology at Loyola University Chicago, Stritch School of Medicine. The terms of this arrangement have been reviewed and approved by Loyola University Chicago in accordance with its conflict of interest policy.

The author Giedrius Kalesnykas, Ph.D. is an employee (CEO) and shareholder of Experimentica Ltd. that offers contract research services employing the preclinical CNV model used in this Article.

## Acknowledgements

The authors would like to thank Yuliya Naumchuk (Loyola University Chicago) and Agne Žiniauskaitė (Experimentica Ltd.) for excellent technical and videographic support. Dr. Kaja's research program is supported by the Dr. John P. and Therese E. Mulcahy Endowed Professorship in Ophthalmology at Loyola University Chicago.

## References

1. Dobi, E. T., Puliafito, C. A., & Destro, M. A new model of experimental choroidal neovascularization in the rat. *Arch. Ophthalmol. Chic. Ill 1960.* **107,** 264-269 (1989).
2. Tobe, T. *et al.* Evolution of neovascularization in mice with overexpression of vascular endothelial growth factor in photoreceptors. *Invest. Ophthalmol. Vis. Sci.* **39,** 180-188 (1998).
3. Seo, M. S. *et al.* Dramatic inhibition of retinal and choroidal neovascularization by oral administration of a kinase inhibitor. *Am. J. Pathol.* **154,** 1743-1753 (1999).
4. Grossniklaus, H. E., Kang, S. J., & Berglin, L. Animal models of choroidal and retinal neovascularization. *Prog. Retin. Eye Res.* **29,** 500-519 (2010).
5. Shah, R. S., Soetikno, B. T., Lajko, M., & Fawzi, A. A. *A* Mouse Model for Laser-induced Choroidal Neovascularization. *J Vis Exp.* (106) e53502 (2015).
6. Giani, A. *et al.* In vivo evaluation of laser-induced choroidal neovascularization using spectral-domain optical coherence tomography. *Invest. Ophthalmol. Vis. Sci.* **52,** 3880-3887 (2011).
7. Gong, Y. *et al.* Optimization of an Image-Guided Laser-Induced Choroidal Neovascularization Model in Mice. *PloS One.* **10,** e0132643 (2015).
8. Sheets, K. G. *et al.* Neuroprotectin D1 attenuates laser-induced choroidal neovascularization in mouse. *Mol. Vis.* **16,** 320-329 (2010).
9. Hoerster, R. *et al.* In-vivo and ex-vivo characterization of laser-induced choroidal neovascularization variability in mice. *Graefes Arch. Clin. Exp. Ophthalmol. Albrecht Von Graefes Arch. Klin. Exp. Ophthalmol.* **250,** 1579-1586 (2012).
10. Sulaiman, R. S. *et al.* A Simple Optical Coherence Tomography Quantification Method for Choroidal Neovascularization. *J. Ocul. Pharmacol. Ther. Off. J. Assoc. Ocul. Pharmacol. Ther.* **31,** 447-454 (2015).

Copyright © 2018 Journal of Visualized Experiments 